In-situ growth of a CdS window layer by vacuum thermal evaporation for CIGS thin film solar cell applications*

Cao Min(曹 敏)[a], Men Chuan-Ling(门传玲)[a]†, Zhu De-Ming(朱德明)[a], Tian Zi-Ao(田子傲)[b], and An Zheng-Hua(安正华)[b]

[a] *School of Energy and Power Engineering, University of Shanghai for Science and Technology, Shanghai* 200093, *China*
[b] *State Key Laboratory of Surface Physics, Department of Physics, Fudan University, Shanghai* 200433, *China*

(Received 18 May 2013; revised manuscript received 20 June 2013)

Highly crystalline and transparent CdS films are grown by utilizing the vacuum thermal evaporation (VTE) method. The structural, surface morphological, and optical properties of the films are studied and compared with those prepared by chemical bath deposition (CBD). It is found that the films deposited at a high substrate temperature (200 °C) have a preferential orientation along (002) which is consistent with CBD-grown films. Absorption spectra reveal that the films are highly transparent and the optical band gap values are found to be in a range of 2.44 eV–2.56 eV. $CuIn_{1-x}Ga_xSe_2$ (CIGS) solar cells with *in-situ* VTE-grown CdS films exhibit higher values of V_{oc} together with smaller values of J_{sc} than those from CBD. Eventually the conversion efficiency and fill factor become slightly better than those from the CBD method. Our work suggests that the *in-situ* thermal evaporation method can be a competitive alternative to the CBD method, particularly in the physical- and vacuum-based CIGS technology.

Keywords: CdS films, CIGS thin film solar cell, vacuum thermal evaporation (VTE), chemical bath deposition (CBD)

PACS: 78.66.Hf, 78.20.Jq, 68.55.J– **DOI:** 10.1088/1674-1056/22/10/107803

1. Introduction

CdS is one of the group II–VI compound semiconductors with a direct optical band gap of ∼ 2.42 eV and can be used as a suitable window layer for $CuIn_{1-x}Ga_xSe_2$ (CIGS) based photovoltaic (PV) devices.[1–7] Based on CdS films, a very high efficiency of CIGS thin film solar cell reaching ∼ 20.3% has been achieved. The energy opto–electric converting interface in the CIGS solar cell is of CdS/CIGS heterostructure.[8–10] The optical and the structural properties of the CdS layer can influence the characteristics of CdS/CIGS heterojunction interface and consequently the performance of the whole PV cell.[11,12]

CdS films have been deposited by various methods such as electro-deposition,[13] molecular beam epitaxy,[14] physical vapor deposition,[15] metal–organic chemical vapor deposition,[16] spray pyrolysis,[17] and chemical bath deposition (CBD).[18] Among these methods, CBD prepared CdS film is widely used for the window layers in CIGS solar cell fabrications because of its low cost and good quality.[2,19–21] Although the CBD process for CdS deposition is very attractive due to its simplicity and the ability to achieve outstanding coverage and good crystalline quality, it tends to form the cubic phase with poor crystalline quality and hence additional annealing process is unavoidable.[22,23] Besides, CBD is a wet chemical method, for industrial production, the wet/dry (vacuum) process is not conducive to CdS/CIGS heterojunction interface. An *in-line* vacuum deposition, e.g., the same vacuum chamber full vacuum dry preparation process, is highly desirable, particularly for physical- and vacuum-based CIGS technology, for example, magnetron sputtering. To the best of our knowledge, the vacuum thermal evaporation (VTE) method is widely used in the preparation of thin film materials because of its low cost, simple process, large area coating, etc. However, VTE method preparation of CdS films is rarely reported.[24]

In the present work, we use an *in-situ* vacuum thermal evaporation (VTE) method to deposit CdS films and investigate their structural, surface morphological, and optical properties, and compare them with those of the standard CBD-deposited films. A complete CIGS thin film solar cell device is prepared in the same vacuum chamber. State-of-the-art device structures including AZO/ZnO/CdS/CIGS/Mo multilayers are fabricated with CdS grown either by *in-situ* VTE or by *ex-situ* CBD and their photo–electric conversion performance are measured.

2. Experimental procedure

CdS films were deposited on glass substrates (dimesions 76 mm×25 mm×1.4 mm) by employing two deposition techniques: VTE and CBD. The substrates were first cleaned with trichloroethylene, acetone, and alcohol. Two VTE copper electrodes were incorporated into the vacuum chamber of a magnetron sputtering system. This allowed the sequential growth of all necessary layers (AZO/ZnO/CdS/CIGS/Mo) in a single vacuum growth chamber and without breaking the vacuum. Tungsten boat was used to evaporate a CdS pow-

*Project supported by the Natural Science Foundation of Shanghai (Grant No. 13ZR1428200).
†Corresponding author. E-mail: anziloveling@126.com
© 2013 Chinese Physical Society and IOP Publishing Ltd

der source with a purity of 99.995% at a base pressure of 4×10^{-3} Pa. Three different substrate temperatures, i.e., room temperature (RT), 100 °C and 200 °C were employed. The deposition rate was regulated to be 0.2 nm/s∼0.4 nm/s. CdS films samples obtained are denoted as VTE-RT, VTE-100, and VTE-200. In the CBD method, chromium sulfate, ammonium chloride, thiourea, and ammonia solution were used to deposit CdS films in a chemical bath at a constant temperature of 85 °C.[25,26] After the growth, CBD–CdS films were further annealed at 400 °C for half an hour. Details of the CBD processes can be found elsewhere.[27–29] The thickness values of the standard VTE–CdS and CBD–CdS films are fixed to be 50 nm for all samples.

For the fabrication of the complete CIGS solar device, a 700-nm Mo bottom contact and a 2-μm CIGS absorption layer were deposited by magnetron sputtering at a substrate temperature of 300 °C. For the growth of CdS window layers, part of the samples were kept in the same chamber and the CdS source was heated thermally. For other samples, they were taken out and immersed into the chemical bath and coated with CdS films by using the CBD method. All devices were completed subsequently by rf-magnetron sputtering ZnO/ZnO: Al transparent bilayers. CIGS battery device samples obtained are denoted as CIGS-RT, CIGS-100, CIGS-200, and CIGS-CBD.

X-ray diffraction (XRD) patterns, SEM images and optical transmission spectra were obtained using an X-ray diffractometer (PANalytical–PW 340/60 X'pert PRO), a field emission scanning electron microscope (FESEM) (HITACHI S-4800), an atomic force microscope (AFM) (Bruker Dimension ICON), and a PerkinElmer UV–vis–NIR double beam spectrophotometer (LAMBDA-35), respectively. Transmission spectra were recorded in a range of 300 nm–1000 nm. The thickness values of the films were measured by employing a profilometer (Surftest SJ-301).

3. Results and discussion

3.1. Structural properties

Figure 1(a) shows the XRD spectra of CdS films deposited by VTE at different substrate temperatures. For comparison, figure 1(b) demonstrates the result from CBD film. As can be seen from Fig. 1(a), the film grown by VTE at RT shows the polycrystalline nature, with (100), (002), and (101) peaks of hexagonal CdS appearing at 24.9063°, 26.6344°, and 28.0447° respectively. As the substrate temperature increases, the (002) diffraction peak becomes most prominent and the intensity is also enhanced while the other peaks almost disappear. This implies that the preferential orientation in the crystalline structure of the VTE films is improved as substrate temperature increases. The preferred orientation of CdS film originates from the controlled nucleation process associated with the low-formation rate of cadmium sulphide.[25,29] The high substrate temperature enables the atoms to travel to their stable locations as desired.[30] Earlier reports indicated that the hexagonal phase CdS is superior to the cubic phase CdS and more suitable as an n-type window layer of CIGS thin film solar cell.[31] The XRD pattern of the CBD–CdS film (Fig. 1(d)) shows a similar peak at $2\theta = 26.64°$, indicating very small difference from that of VTE-200. It is noteworthy to point out that no additional heat treatment was carried out for VTE films while the CBD films were post-annealed to achieve the anticipated hexagonal (002) preferential orientation.

The average grain sizes (D) of the CdS films deposited at different substrate temperatures were calculated using Scherrer's formula[32]

$$D = \frac{0.9\lambda}{\beta\cos\theta}, \tag{1}$$

where λ, β, and θ are X-ray wavelength (1.541), full width of half maximum (FWHM) of the (002) peak, and the Bragg diffraction angle, respectively. The average grain size of the VTE films is found to increase from 45 nm∼75 nm with substrate temperature increasing. This suggests that microcrystalline grain regrows during the film deposition, improving the crystallinities of the films. The grain size of CBD–CdS film estimated from the (002) peak of XRD pattern (Fig. 1(d)) is ∼ 50 nm. These calculated results are included and compared in Table 1.

Table 1. Structural and optical parameters of the CdS films with the values of thickness (t), full width at half maximum (β), grain size (D), and the roughness (R).

Sample	t/nm	$\beta/10^{-3}$ rad	D/nm			R/nm (from AFM)
			XRD	SEM	AFM	
VTE (RT)	50	3.647	52	40–60	53	4.2
VTE (100°)	50	3.269	58	50–70	59	4.4
VTE (200°)	50	2.874	66	55–75	68	4.3
CBD	50	3.804	50	40–60	51	9.6

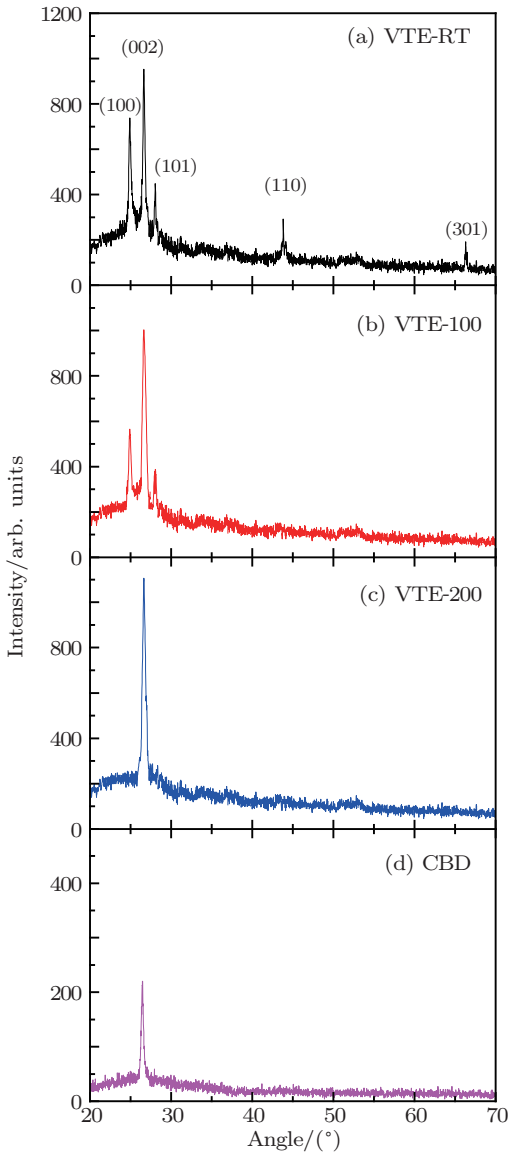


Fig. 1. (color online) XRD spectra of CdS thin films deposited by VTE at different substrate temperatures, marked by VTE-RT (a), VTE-100 (b), VTE-200 (c). For comparison, panel (d) shows the result from CBD film.

3.2. Surface properties

The FESEM images of the films are shown in Fig. 2, and the grain size values of VTE-RT, VTE-100, and VTE-200 are found to be in ranges of 40 nm∼55 nm, 50 nm∼65 nm, and 55 nm∼75 nm, respectively. Obviously, the CdS grains deposited by VTE are much larger than those of CBD–CdS film (Fig. 2(d)). These results are in good consistence with those calculated from the XRD results.

As a window layer, the CdS layer is required to be free of holes with uniform coverage which considerably affects the performance of the final device.[33] In this regard, all of the films appear to be rather smooth with well-defined and round shaped grains.[34,35] In Fig. 2(d), it can be seen that the grains of the CBD–CdS films are tightly packed and have smaller and more uniform grain size. To derive root-mean-square (RMS) roughness (R) data, AFM images are acquired and shown in Fig. 3. Table 1 indicates the values of the RMS roughness value (R) and grain size (D) of VTE–CdS and CBD–CdS films. From Table 1, the grain sizes of VTE–CdS films deposited at RT are nearly the same as those of CBD–CdS films. With the increase of substrate temperature, the grain sizes of the VTE–CdS films increase. On the other hand, the average roughness values of VTE–CdS films are in a range of 4.2 nm∼4.4 nm with little dependence on substrate temperature. It is a little surprising that the average roughness value of CBD–CdS films appears to be considerably larger (~ 9.6 nm). This might come mainly from the larger gaps between neighboring grains which could appear as a consequence of chemical decomposition of complex residual substances during the high temperature annealing.

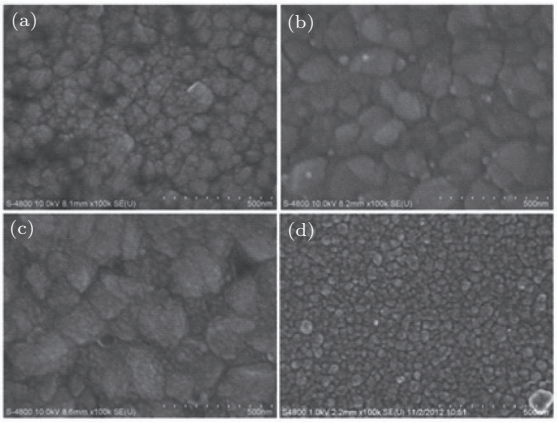


Fig. 2. FESEM images of CdS thin film samples denoted as (a) VTE-RT, (b) VTE-100, (c) VTE-200, and (d) CBD.

3.3. Optical properties

The optical transmittance spectra of different CdS films are shown in Fig. 4. All samples with a thickness of 50 nm show good transmission ($> 80\%$) for wavelengths larger than 550 nm, which is one of the prerequisites for window layers in solar optoelectronic devices.[30] As shown in Fig. 4, the absorption edge[36] of CdS film deposited by VTE becomes steeper with the increase of substrate temperature. Particularly, all of them are sharper than CBD samples. The sharper absorption edge indicates that the CdS film has fewer defect states and better crystallization quality, as a result, suppressing the recombination loss of the optical carriers.

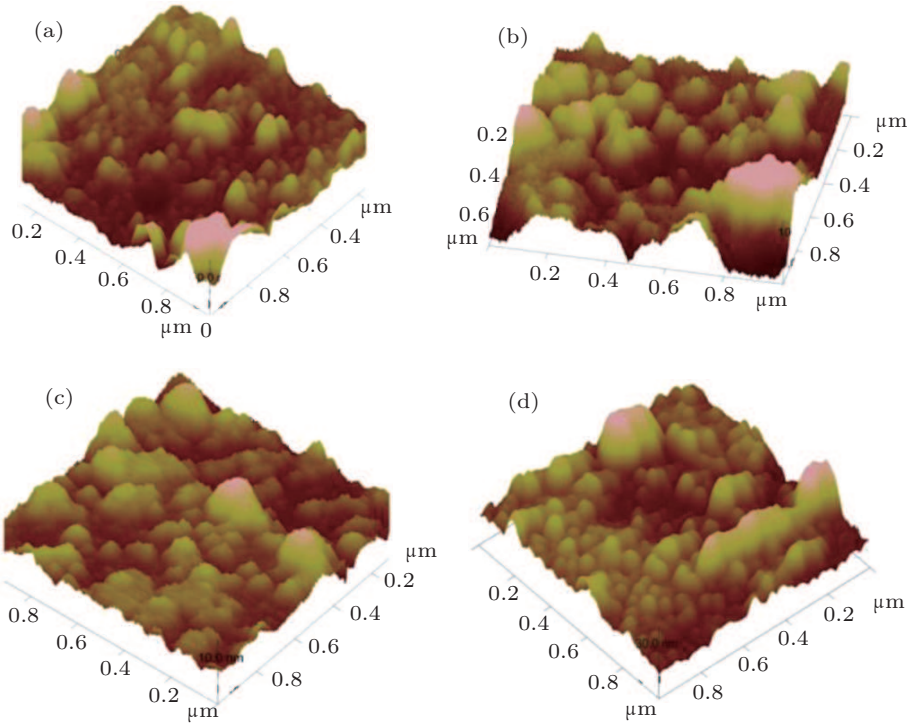


Fig. 3. (color online) AFM images of CdS film samples denoted as (a) VTE-RT, (b) VTE-100, (c) VTE-200, and (d) CBD.

The dependence of the absorption coefficient α on the incident photon energy $h\nu$, in semiconductors takes the form,[37]

$$\alpha h\nu = \kappa(h\nu - E_g)^{n/2}, \tag{2}$$

where E_g is the optical band gap, k is a constant related to the effective mass associated with the band, and n is a constant which is equal to one for a direct-gap material and four for an indirect-gap material.

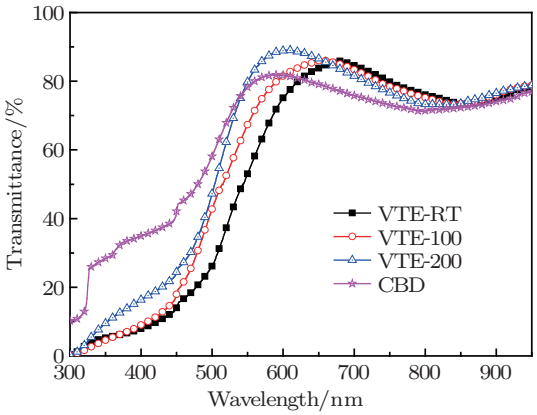


Fig. 4. (color online) Absorption spectra of 50-nm-thick CdS thin films denoted as VTE-RT, VTE-100, VTE-200, and CBD.

To determine whether the CdS films deposited using VTE have direct or indirect band gap, $(\alpha h\nu)^2$ versus $h\nu$ and $(\alpha h\nu)^{1/2}$ versus $h\nu$ plots were drawn. Better linearity is obtained in the $(\alpha h\nu)^2$ versus $h\nu$ plot as shown in Fig. 5. Therefore, the direct bandgap values are determined by extrapolating the linear portion of these plots to the energy axis and the derived E_g values are presented in the inset of Fig. 5. With the increase of substrate temperature, the VTE samples show larger slope and therefore larger E_g. Interestingly, CBD films show largest E_g but with serious band-tail absorption which may arise from the high defect states around grain boundaries.

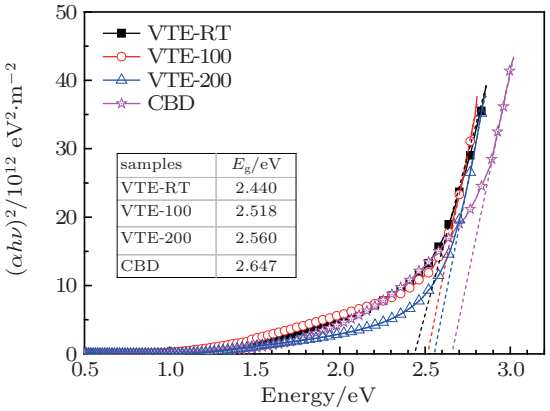


Fig. 5. (color online) Bandgap derivations of CdS thin films deposited by VTE and CBD methods, denoted as VTE-RT, VTE -100, VTE-200, and CBD.

3.4. Electrical properties

Current–voltage (J–V) curves of fabricated CdS/CIGS solar cells at different substrate temperatures are shown in Fig. 6. It is found that with the increase of substrate temperature, the short-circuit current density (J_{sc}) of VTE devices increases considerably and the open circuit voltage (V_{oc}) also increases slightly. This may be attributed to the higher preferential orientation and larger grain size in high temperature

sample.[38] As a comparison, the CBD device shows small V_{oc} and large J_{sc}. To make an analytical analysis, we consider the analytic expression of the open circuit voltage V_{oc} as shown in the following[39]

$$V_{oc} = \frac{E_g}{q} - \frac{KT \ln\left(\frac{N_c N_v D_n q}{J_{sc} h L_n}\right)}{q}, \quad (3)$$

where E_g is band-gap of the absorption layer (i.e., CIGS), D_n is the diffusion constant for electrons, $N_{c/v}$ is the effective density of states in the conductance/valence band, h is the acceptor density, and L_n is the diffusion length of the electrons which depends on recombination rate. Since E_g (of the CIGS absorption layer) is common for all devices, it is mainly influenced by L_n or the recombination, according to Eq. (3). In the CBD device, defect states suppress L_n (as implied by the large band tail absorption in Fig. 4 and the high interfacial area in Fig. 2) and therefore a lower V_{oc} is obtained. As to J_{sc}, it is uncertain why the VTE device exhibits lower J_{sc}, but we surmise that it is related to the poorer surface coverage for thin CdS film with larger grain size. Alternatively, the Cd^{2+} ion diffusion in the CBD process may improve the interfacial contact and therefore reduce the series resistance which eventually leads to higher J_{sc}.

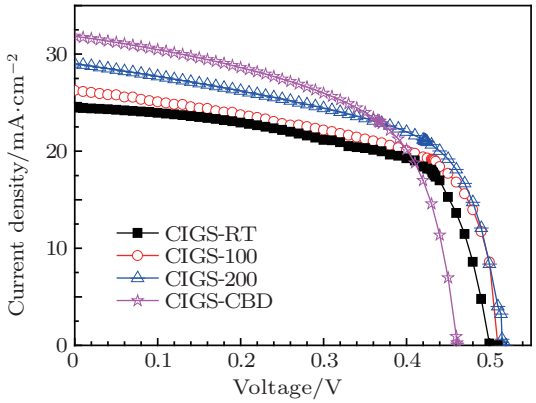


Fig. 6. (color online) *J–V* characteristics of CdS/CIGS solar cells with different CdS films.

Table 2 summarizes the device performances of all the solar cells. Of them, the sample of CIGS-200 shows the best performance. The open circuit voltage (V_{oc}) and the conversion efficiency are 515 mV, and 4.45%, respectively, which are significantly higher than those of the other samples.

Table 2. Performances of CdS/CIGS solar cells with different CdS films by VTE and CBD.

Samples	V_{oc}/mV	I_{sc} /mA·cm^{-2}	Fill factor/%	Efficiency/%
CIGS-RT	507	24.46	54.8	4.03
CIGS-100	510	26.26	57.6	4.07
CIGS-200	515	29.1	59.6	4.45
CIGS-CBD	461	31.85	60.0	4.23

4. Conclusions

A simple and *in-situ* vacuum thermal evaporation (VTE) technique is employed to fabricate CdS films. At a high substrate temperature, good CdS window layer with large grain sizes, highly preferential orientation of hexagonal (002), good optical transparency, and surface properties can be obtained. The CdS/CIGS solar cells with VTE CdS films have achieved better performance (efficiency = 4.45%, $J_{sc} = 29.1$ mA/cm^2, $V_{oc} = 515$ mV, and $FF = 59.6\%$). We believe that the better compatibility with the present vacuum-based CIGS technology makes the VTE a promising candidate in future industrial applications.

Acknowledgment

Some of the measurements were supported by the Institute of Advanced Materials of Fudan University, China.

References

[1] Chen D S, Yang J, Zhou P H, Du H W, Shi J W, Yu Z S, Zhang Y H, Brian B and Ma Z Q 2013 *Chin. Phys. B* **22** 018801
[2] Sho S, Katsuhiko O, Yasuyuki I and TOkio N 2009 *Solar Energy Mater. Solar Cell.* **93** 988
[3] Sakurai T, Ishida N, Ishizuka S, Isiam M M, Kasai A, Matsubara K, Sakurai K, Yamada A, Akimoti K and Niki S 2008 *Thin Solid Films* **516** 7036
[4] Hariskos D, Powalla M, Chevaldonnet N, Lincot D, Chindler A S and Dimmler B 2001 *Thin Solid Films* **387** 179
[5] Contreras M A, Romero M J, To B, Hasoon F, Nonfi R, Ward S and Ramanathan K 2002 *Thin Solid Films* **403–404** 204
[6] Chung Y D, Cho D H, Choi H W, Lee K S, Ahn B J, Song J H and Kim J 2012 *J. Kor. Phys. Soc.* **61** 1623
[7] Men C L, Tian Z A, Shao Q P, Zhang H and An Z H 2012 *Appl. Surf. Sci.* **258** 10195
[8] Xavier M, Pantoja J E, Alessandro R and Ayodhya N T 2004 *Solar Energy* **77** 831
[9] Antonio L and Steven H 2003 *Handbook of Photovoltaic Science and Engineering*, 2nd edn. (England: John Wiley & Sons Ltd), Chapter 14
[10] Li B, Feng L H, Wang Z, Zheng X, Zheng J G, Cai Y P, Zhang J Q, Li W, Wu L L, Lei Z and Zeng G G 2011 *Chin. Phys. B* **20** 037103
[11] Miguel A C, Manuel J R, Bobby and Hasoon F 2002 *Thin Solid Films* **403** 204
[12] Touskova J, Kindl D, Dobiasova L and Tousek J 1998 *Solar Energy Mater. Solar Cells* **53** 177
[13] Sasikala G, Dhnasekaran R and Subramanian C 1997 *Thin Solid Films* **302** 71
[14] Brunthaler G, Lang M, Forstner A, Giftge C, Schikora D, Fereira S, Sitter H and Lischka K 1994 *J. Crystal Growth* **138** 559
[15] Birkmire R W, McCandless B E and Shafarman W N 1988 *Solar Energy* **23** 115
[16] Chou H C and Ohatgi A R 1994 *Electron. Mater.* **23** 31
[17] Mathew S, Mukerjee P S and Vijayakumar K P 1995 *Thin Solid Films* **254** 278
[18] Zhang H, Ma X and Yang D 2003 *Mater. Lett.* **58** 5
[19] Xu C M, Sun Y, Zhou L, Li F Y, Zhang L, Xue Y M, Zhou Z Q and He Q 2006 *Chin. J. Semicond.* **23** 2259
[20] Takashi M, Takuya M, Hideyuki T, Yoshihiro H, Takayuki N, Yasuhiro H, Takashi U and Masatoshi K 2001 *Solar Energy Mater. & Solar Cells* **67** 83
[21] Raviprakash Y, BangeraaKasturi V and Shivakumara G G 2010 *Curr. Appl. Phys.* **10** 193
[22] Ferekides C, Marinksiy D and Morel D L 1997 *Proceedings of the* 26*th IEEE Photovoltaic Specialists Conference,* September 30–October 3, 1991, Anaheim, USA, p. 339

[23] Durose K, Edwards P R and Halliday D P 1999 *J. Crystal Growth* **197** 733
[24] Shan Y Q, Dang P and Yu X Z 2009 *Journal of Northeastern University* **30** 392
[25] Li W Y, Cai X, Chen Q L and Zhou Z B 2005 *Mater. Lett.* **59** 1
[26] Tokio N 2005 *Thin Solid Films* **480–481** 419
[27] Kaur I, Pandya D K and Chopra K L 1980 *Electrochem. Soc.* **12** 943
[28] Elangovan E and Ramamurthi K 2005 *Appl. Surf. Sci.* **249** 183
[29] Sharama S N, Sharma R K, Sood K N and Singh S 2005 *Mater. Chem. Phys.* **93** 368
[30] Kim Y J, Kin Y T, Yang H J, Park J C, Han J I, Lee Y E and Kim H J 1997 *Vac. Sci. Technol. A* **15** 1103
[31] Subba R K, Pilkington R D and Hill A E 2001 *Mater. Chem. Phys.* **68** 22
[32] Atay F, Bilgin V, Akyuz I and Kose S 2003 *Mater. Sci. Semicond. Proc.* **6** 197
[33] Lee J 2005 *Appl. Surf. Sci.* **252** 1398
[34] Ravichandran K and Philominathan P 2009 *Appl. Surf. Sci.* **255** 5736
[35] Wang Z J, Song L J, Li S C, Lu Y M, Tian Y X, Liu J Y and Wang L Y 2006 *Chin. Phys.* **15** 2710
[36] Wang M D, Zhu D Y, Liu Y, Zhang L, Zheng C X, He Z H, Chen D H and Wen L S 2008 *Chin. Phys. Lett.* **25** 743
[37] Moon B, Lee J and Jung H 2006 *Thin Solid Films* **511** 299
[38] Green M A 1981 *Solar Cells: Operating Principles, Technology, and System Applications* (Englewood Cliffs: Prentice-Hall)
[39] Peter W and Uli W 2005 *Physics of Solar Cells: From Basic Principles to Advanced Concepts* (Gmbh & Co. kGaA: Wiley-VCH Verlag) p. 1